PERGAMON

International Journal of Heat and Mass Transfer 42 (1999) 1383–1388

International Journal of HEAT and MASS TRANSFER

Laminar mixed convection correlations for an isothermal cylinder in cross flow at different angles of attack

Bassam A./K. Abu-Hijleh*

Mechanical Engineering Department, Jordan University of Science and Technology, P.O. Box 3030, Irbid 22110, Jordan

Received 23 October 1997; in final form 6 August 1998

Abstract

The problem of laminar mixed convection from an isothermal cylinder is solved numerically. The average Nusselt number is calculated at different values of Reynolds number, Grashof number, and incoming free stream angle of attack. Different correlations are presented, each valid for a specific range of Reynolds number, buoyancy parameter, and angle of attack.

Nomenclature

D cylinder diameter, $2r_0$
E parameter in computational domain, $\pi e^{\pi\xi}$
g gravity
Gr Grashof number based on cylinder radius, $g\beta(T_0-T_\infty)r_0^3/\nu^2$
Gr_D Grashof number based on cylinder diameter, $g\beta(T_0-T_\infty)D^3/\nu^2$
h local convection heat transfer coefficient
k conduction heat transfer coefficient
M number of grid points in the tangential direction
N number of grid points in the radial direction
$\overline{Nu}$ average Nusselt number based on cylinder diameter, eqn (6)
P non-dimensional pressure
p pressure
Pr Prandtl number
R non-dimensional radius
r radius
Re Reynolds number based on radius, $U_\infty r_0/\nu$
Re_D Reynolds number based on diameter, $U_\infty D/\nu$
T temperature
U non-dimensional radial velocity
u radial velocity
V non-dimensional tangential velocity
v tangential velocity.

Greek symbols
α thermal diffusivity
β coefficient of thermal expansion
γ angle of attack of incoming free stream flow
$\in$ measure of convergence of numerical results
η independent parameter in computational domain representing tangential direction
θ angle
κ buoyancy parameter, Gr_D/Re_D^2
λ correlation parameter used in eqns (18)–(22), $\kappa^{0.2335}Re_D^{0.06793}$
ν kinematic viscosity
ξ independent parameter in computational domain representing radial direction
ρ density
ϕ non-dimensional temperature
ψ stream function
ω vorticity function.

Subscripts
D value based on cylinder diameter
f value due to forced convection
m value due to mixed convection, arbitrary angle of attack
m0 value due to mixed convection, cross flow case
0 value at cylinder surface
∞ free stream value.

1. Introduction

The laminar convection from a heated cylinder is an important problem in heat transfer. It is used to simulate

* Tel.: 00962 2 295111ex2572; fax: 00962 2 295018; e-mail: bassam@just.edu.jo

0017–9310/98/$ - see front matter
PII: S0017–9310(98)00249–X

a wide range of engineering applications as well as provide a better insight into more complex systems of heat transfer. Most of the empirical formulas that exist are for either pure-forced or pure-natural convection. There are several cases where the contribution of both modes of heat transfer is of the same order. This case is referred to as mixed convection. Some researchers did study the problem but limited themselves to either cross flow only [1-4] or assisting only [5]. Hatton et al. [6] reported on mixed convection at three angles of attack: 90° (aiding), 0° (cross), and −90° (opposing). The results were not consistent in the mixed convection region, i.e. the range where the forced and natural convection were of the same order. Badr [7] proposed separate correlations for cross, aiding, and opposing mixed convection from a horizontal cylinder based on numerical simulation. The data was for low Reynolds number, Re_D 5–60, and moderate buoyancy parameter, κ 0–4. Morgan [8] compiled a wide range of experimental data that covered the full range of natural, mixed, and forced convection from a cylinder. The data did include results at different positive angles of attack as reported by different researchers. There was a great deal of discrepancy in the data reported. Morgan [8] did not suggest any correlation for these cases. To the best knowledge of the author, there is no correlation, in the open literature, that handles mixed convection at arbitrary angles of attack. This was the motivation for this study.

2. Mathematical analysis

The steady-state equations for the 2-D laminar mixed convection over a cylinder, including the Boussinesq approximation, are given by:

$$\frac{1}{r}\frac{\partial(ru)}{\partial r}+\frac{1}{r}\frac{\partial v}{\partial\theta}=0 \tag{1}$$

$$u\frac{\partial u}{\partial r}+\frac{v}{r}\frac{\partial u}{\partial\theta}-\frac{v^2}{r}=\frac{1}{\rho}\left[\rho g\beta(T-T_\infty)\sin(\theta)-\frac{\partial p}{\partial r}\right]+\nu\left[\frac{\partial^2 u}{\partial r^2}+\frac{1}{r}\frac{\partial u}{\partial r}-\frac{u}{r^2}+\frac{1}{r^2}\frac{\partial^2 u}{\partial\theta^2}-\frac{2}{r^2}\frac{\partial v}{\partial\theta}\right] \tag{2}$$

$$u\frac{\partial v}{\partial r}+\frac{v}{r}\frac{\partial v}{\partial\theta}+\frac{uv}{r}=\frac{1}{\rho}\left[\rho g\beta(T-T_\infty)\cos(\theta)-\frac{1}{r}\frac{\partial p}{\partial\theta}\right]+\nu\left[\frac{\partial^2 v}{\partial r^2}+\frac{1}{r}\frac{\partial v}{\partial r}-\frac{v}{r^2}+\frac{1}{r^2}\frac{\partial^2 v}{\partial\theta^2}+\frac{2}{r^2}\frac{\partial u}{\partial\theta}\right] \tag{3}$$

$$u\frac{\partial T}{\partial r}+\frac{v}{r}\frac{\partial T}{\partial\theta}=\alpha\nabla^2 T \tag{4}$$

where

$$\nabla^2\equiv\left[\frac{\partial^2}{\partial r^2}+\frac{1}{r}\frac{\partial}{r\partial r}+\frac{1}{r^2}\frac{\partial^2}{\partial\theta^2}\right] \tag{5}$$

Equations (1)–(4) are subject to the following boundary conditions:

1. On the cylinder surface, i.e. $r=r_0$; $u=v=0$ and $T=T_0$.
2. Far-stream from the cylinder, i.e. r→∞; $u\to U_\infty\cos(\theta-\gamma)$ and $v\to -U_\infty\sin(\theta-\gamma)$. For the temperature, T, the far-stream boundary condition is divided into an inflow ($\pi/2\leqslant(\theta-\gamma)\leqslant 3\pi/2$) and an outflow ($0\leqslant(\theta-\gamma)<\pi/2$ & $3\pi/2<(\theta-\gamma)\leqslant 2\pi$) regions (Fig. 1). The far-stream temperature boundary conditions are $T\to T_\infty$ and $\partial T/\partial r\to 0$ for the inflow and outflow regions, respectively.

The average Nusselt number, based on diameter, is calculated as:

$$\overline{Nu}=\frac{1}{2\pi}\frac{D}{k}\int_0^{2\pi}h(\theta)\,\mathrm{d}\theta=-\frac{D}{2\pi}\int_0^{2\pi}\frac{\partial T(r_0,\theta)/\partial r}{(T_0-T_\infty)}\partial\theta \tag{6}$$

The following non-dimensional groups are introduced:

$$R\equiv\frac{r}{r_0},\ U\equiv\frac{u}{U_\infty},\ V\equiv\frac{v}{U_\infty},\ \phi\equiv\frac{(T-T_\infty)}{(T_0-T_\infty)},\ P\equiv\frac{(p-p_\infty)}{\frac{1}{2}\rho U_\infty^2}$$

Using the steam function–vorticity formulation, the non-dimensional form of eqns (1)–(4) are given by:

$$\omega=\nabla^2\psi \tag{7}$$

$$U\frac{\partial\omega}{\partial R}+\frac{V}{R}\frac{\partial\omega}{\partial\theta}=\frac{1}{Re}\nabla^2\omega-\frac{Gr}{Re^2}\left[\cos(\theta)\frac{\partial\phi}{\partial R}-\frac{1}{R}\sin(\theta)\frac{\partial\phi}{\partial\theta}\right] \tag{8}$$

$$U\frac{\partial\phi}{\partial R}+\frac{V}{R}\frac{\partial\phi}{\partial\theta}=\frac{1}{RePr}\nabla^2\phi \tag{9}$$

where

$$U\equiv\frac{1}{R}\frac{\partial\psi}{\partial\theta},\quad V\equiv-\frac{\partial\psi}{\partial R} \tag{10}$$

The new non-dimensional boundary conditions for eqns (7)–(9) are given by:

1. On the cylinder surface, i.e. $R=1.0$; $\psi=\partial\psi/\partial R=0$, $\omega=\partial^2\psi/\partial R^2$, and $\phi=1.0$.
2. Far-stream form the cylinder, i.e. $R\to\infty$; $1/R$

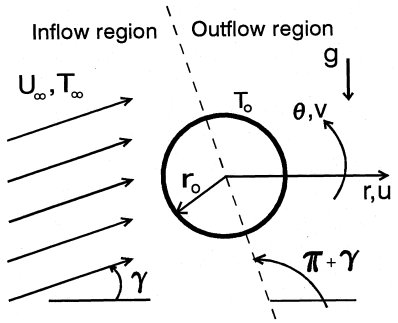

Fig. 1. Schematic of the flow field and physical parameters.

$(\partial\psi/\partial\theta) = \cos(\theta-\gamma)$ and $(\partial\psi/\partial R) = \sin(\theta-\gamma)$. For the non-dimensional temperature, $\phi = 0$ and $(\partial\phi/\partial R) = 0$, for the inflow and outflow, respectively.

In order to accurately resolve the boundary layer around cylinder, a grid with small radial spacing is required. It is not practical to use this small spacing as we move to the far-stream boundary. Thus a stretched grid in the radial direction is needed [9]. This will result in unequally spaced nodes and would require the use of more complicated and/or less accurate finite difference formulas. To overcome this problem, the unequally spaced grid in the physical domain (R,θ) is transformed into an equally spaced grid in the computational domain (ξ,η) [9], Fig. 2. The two domains are related as follows:

$$R = e^{\pi\xi}, \theta = \pi\eta \tag{11}$$

Equations (7)–(9) along with the corresponding boundary conditions need to be transformed into the computational domain. In the new computational domain, the curent problem will be given by:

$$\omega = \frac{1}{E^2}\left[\frac{\partial^2\psi}{\partial\xi^2} + \frac{\partial^2\psi}{\partial\eta^2}\right] \tag{12}$$

$$\frac{\partial^2\omega}{\partial\xi^2} + \frac{\partial^2\omega}{\partial\eta^2} = \frac{1}{Re}\left[\frac{\partial\psi}{\partial\eta}\frac{\partial\omega}{\partial\xi} - \frac{\partial\psi}{\partial\xi}\frac{\partial\omega}{\partial\eta}\right] + E\frac{Gr}{Re^2}\left[\cos(\pi\eta)\frac{\partial\phi}{\partial\xi} - \sin(\pi\eta)\frac{\partial\phi}{\partial\eta}\right] \tag{13}$$

$$\frac{\partial^2\phi}{\partial\xi^2} + \frac{\partial^2\phi}{\partial\eta^2} = \frac{1}{RePr}\left[\frac{\partial\psi}{\partial\eta}\frac{\partial\phi}{\partial\xi} - \frac{\partial\psi}{\partial\xi}\frac{\partial\phi}{\partial\eta}\right] \tag{14}$$

where

$$E = \pi e^{\pi\xi} \tag{15}$$

The transformed boundary conditions are given by:

1. On the cylinder surface, i.e. $\xi = 0$; $\psi = \partial\psi/\partial\xi = 0$, $\omega = (1/\pi^2)\partial^2\psi/\partial\xi^2$, and $\phi = 1.0$.
2. Far-stream form the cylinder, i.e. $\xi\to\infty$; $\partial\psi/\partial\xi = E\sin(\theta-\gamma)$. In the inflow region; $\omega\to 0$ and $\phi\to 0$. In the outflow region; $\partial\omega/\partial\xi\to 0$ and $\partial\phi/\partial\xi\to 0$.

The elliptic system of PDEs given by eqns (12)–(14) along with the corresponding boundary conditions was discretized using finite difference method. The resulting system of algebraic equations was solved using an explicit hybrid scheme [10]. Such a method proved to be numerically stable for convection-diffusion problems. The finite difference form of the equations was checked for consistency with the original PDEs [8]. The iterative solution procedure was carried out until the error in all solution variables (ψ,ω,ϕ) became less than a predefined error level (ϵ). Other predefined parameters needed for the solution method included the placement of the far-stream boundary condition (R_∞) and the number of grid points in both radial and tangential directions, N and M, respectively. Extensive testing was carried out in order to determine the effect of each of these parameters on the solution. This was done to ensure that the solution obtained was independent of and not tainted by the predefined value of each of these parameters. The testing included varying the value of ϵ from 10^{-3} to 10^{-6}, R_∞ from 5 to 50, N from 60 to 150, and M from 60 to 144. The results reported herein are based on the following combination: $N = 100$, $M = 120$, $R_\infty = 20$, and $\epsilon = 10^{-4}$. The current grid resolution used is better than most grids used in published studies of forced convection from a heated cylinder [11].

3. Results

The goal of this study is to come up with a correlation that can be used to predict the Nusselt number, $\overline{Nu}_m$, due

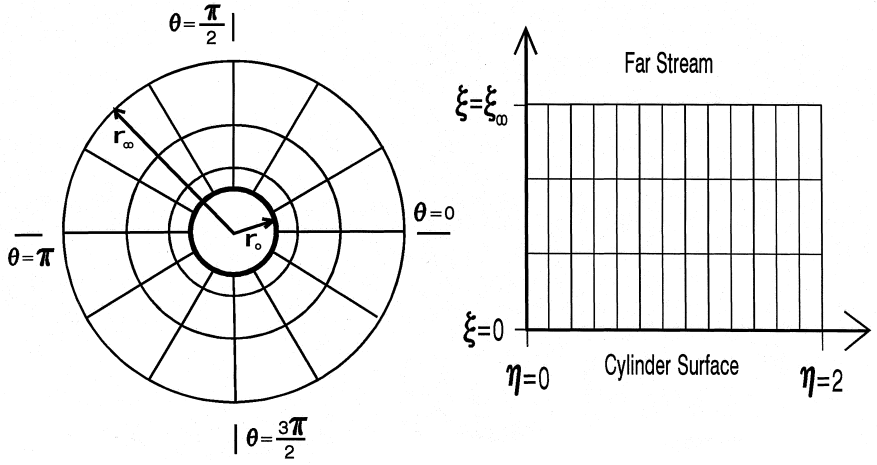

Fig. 2. Schematic of the finite difference grid in the physical (left) and the computational (right) domains.

to mixed convection from an isothermal cylinder at arbitrary angles of attack. The fluid under consideration is air, $Pr = 0.71$. This will be done in three steps. First, a correlation for pure forced convection is sought. Next, we seek a correlation for normalized Nusselt number in mixed convection due to cross flow ($\gamma = 0$), $\overline{Nu_{m0}}/\overline{Nu_f}$. Finally, we seek a general correlation for normalized Nusselt number in mixed convection at arbitrary angles of attack, $\overline{Nu_m}/\overline{Nu_{m0}}$. To achieve this goal, the combination of a wide range of Re_D, κ, and γ was studied. The values used were: Re_D (1, 5, 10, 20, 40, 60, 80, 100, 200), κ (0, 0.2, 0.5, 1, 5, 10, 20, 35) and γ (degrees) (-90, -75, -60, -45, -30, -20, -10, -5, 0, 5, 10, 20, 30, 45, 60, 75, 90). The current study included more than 1200 different computer runs, including more than 50 runs for code validation. The code was written using MS Power Station 32-bit Fortran compiler. Double precision was used for all variables in the code. The code took between 2 and 5 h on a Pentium PC, depending on the value of the parameters involved.

The two most common correlation forms for $\overline{Nu_f}$ are: $\overline{Nu_f} = a + b^* Re_D^c$ and $\overline{Nu_f} = b^* Re_D^c$. Linear regression was used to find the best combination of constants for each form based on the numerical results predicted by the present study. The two new correlations are given by:

$$\overline{Nu_f} = 0.3174 + 0.5439 Re_D^{0.4556}; \quad 1 \leqslant Re_D \leqslant 200 \tag{16}$$

$$\overline{Nu_f} = 0.7289 Re_D^{0.4079}; \quad 1 \leqslant Re_D \leqslant 200 \tag{17}$$

The correlation given by eqn (16) proved to be more accurate than that of eqn (17). The maximum and average relative errors between the correlation and numerical data were: 0.8% @ $Re_D = 1$ and 0.4%, and 14.7% @ $Re_D = 1$ and 2.7%, for eqns (16) and (17), respectively. Figure 3 includes the variation of $\overline{Nu_f}$ at different values of Re_D as predicted by several published empirical formulas [3, 4, 11, 12], experimental data [2, 13], the current numerical data, and eqn (16). The results of the references empirical formulas were restricted to their applicable range of Re_D. The results of the present study compare well with the published results.

Figure 4 shows the change in $\overline{Nu_{m0}}/\overline{Nu_f}$ due to cross flow, i.e. $\gamma = 0$, at different values of buoyancy parameter $\kappa \equiv Gr_D/Re_D^2$) and Re_D. At low ReD and κ, $\overline{Nu_{m0}}/\overline{Nu_f}$ was slightly less than 1.0. This phenomena was observed experimentally by Hatton et al. [7] and numerically by Ahmad and Qureshi [4]. At low Re_D, the boundary layer is thick. This caused the program to crash for large values of κ. Thus the results shown for the cases of $Re_D = 1$ and 5 were limited to $\kappa = 10$ and 20, respectively. The curves for different values of Re_D do not collapse. This indicates that $\overline{Nu_{m0}}/\overline{Nu_f}$ does not correlate with just κ. Thus a new correlation parameter was sought. The form of the new parameter, λ, was chosen based on least square regression fit of the current results. The fact that $\overline{Nu_{m0}}/\overline{Nu_f}$ did not correlate with the traditional buoyancy parameter, κ, can be attributed to the averaging effect of κ, where κ is an indication of the average relative magnitude of the buoyancy force to the inertia force, but the intertia force is not uniform around the cylinder. Also, the size and strength of the wake behind the cylinder depends on the incoming Re_D. This will cause the buoyancy force to have different local effects on flow for different Reynolds numbers even though the overall buoyancy parameter is the same. Based on the data shown in Fig. 4, the following correlation for mixed convection due to cross flow is proposed:

$$\frac{\overline{Nu_{m0}}}{\overline{Nu_f}} = 1.002 - 0.2194\lambda + 0.2298\lambda^{1.743}; \quad 1 \leqslant Re_D \leqslant 200, 0 \leqslant \kappa \leqslant 35 \tag{18}$$

where

$$\lambda \equiv \kappa^{0.2335} Re_D^{0.06793} \tag{19}$$

The maximum and average relative errors between the cross-flow mixed convection correlation and numerical data were: 4.3% @ ($Re_D = 100$ and $\kappa = 5$) and 1.4%, respectively. In general the error was significant at the high values of Re_D and/or high values of κ. The negative sign of the second term in eqn (18) gives rise to values of

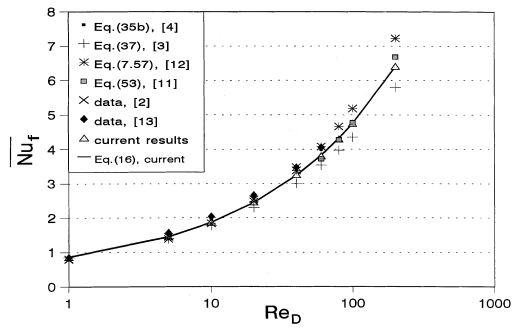

Fig. 3. Variation of Nusselt number with Reynolds number due to forced convection.

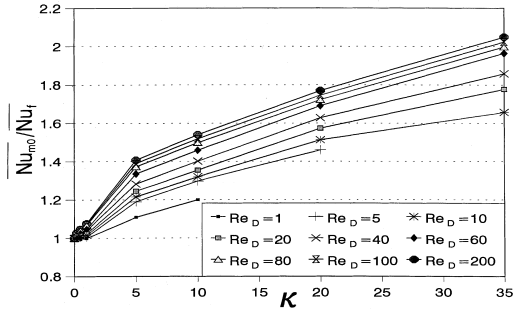

Fig. 4. Variation of normalized Nusselt number with buoyancy parameter due to cross flow mixed convection.

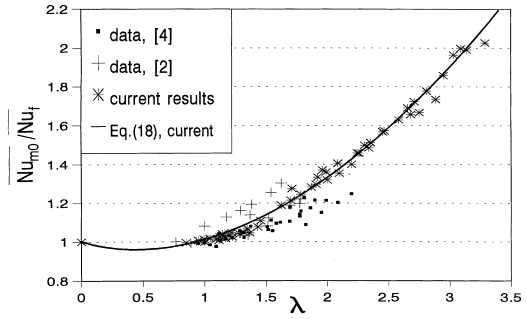

Fig. 5. Data points and correlation of normalized Nusselt number due to cross flow mixed convection.

$\overline{Nu_{m0}}/\overline{Nu_f} < 1.0$ at low values of λ. Figure 5 shows $\overline{Nu_{m0}}/\overline{Nu_f}$ vs λ from the current study, the data of Badr [2] and Ahmad and Qureshi [4], as well as the correlation given by eqn (18). The current results and the new correlation compare well with the published data.

Next came the difficult task of correlating the change in Nusselt number at different Re_D, κ, and γ. The correlation sought was in the form of $\overline{Nu_m}/\overline{Nu_{m0}}$. The best correlation obtained when all data points were taken into consideration is as follows:

$$\frac{\overline{Nu_m}}{\overline{Nu_{m0}}} = [0.9826 + 0.4588\lambda^{0.1235}\sin(\gamma)]^{0.3599};$$
$$1 \leqslant Re_D \leqslant 200, 0 \leqslant \kappa \leqslant 35 \quad (20)$$

Figure 6 shows the data from Badr [6], the curent numerical results, and the predictions of eqn (20). The current results match the data reported by Badr [6] and show that changing the angle of attack can result in a $+20\%$ to -30% change in the average Nusselt number compared to the case of cross flow. Figure 6 shows a substantial difference between the data from Bard [6], the curent numerical results, and the prediction at the low end of the x-axis. This corresponds to cases of high κ and low γ values approaching $-\pi$, i.e. opposing flow. The maximum and average relative errors between the correlation given by eqn (20) and numerical data were: 28.3 and 3.2%, respectively. The main cause for this problem is the way the boundary conditions are defined at the inflow region. For the case of high κ, the plume will exit the computational domain across the arc designated as an inflow region. At this point the velocity generated by the buoyancy effect in the plume will be in the direction opposite to that of the incoming free stream flow. These conflicting conditions would affect the numerical results.

With this in mind, two other correlations, each with its own more restrictive range of applicability, are proposed. The first is limited to low values of κ while the second is limited to positive angles of attack. Both correlations are applicable to the range $1 \leqslant Re_D \leqslant 200$. The new correlations are:

$$\frac{\overline{Nu_m}}{\overline{Nu_{m0}}} = [0.9766 + 0.4023\lambda^{0.3995}\sin(\gamma)]^{0.3853};$$
$$0 \leqslant \kappa \leqslant 10, -\pi \leqslant \gamma \leqslant \pi \quad (21)$$

$$\frac{\overline{Nu_m}}{\overline{Nu_{m0}}} = [0.9995 + 0.3605\lambda^{0.2237}\sin^{0.8053}(\gamma)]^{0.3820};$$
$$0 \leqslant \kappa \leqslant 35, 0 \leqslant \gamma \leqslant \pi \quad (22)$$

Figures 7 and 8 show a comparison between the numerical results and the correlations for the cases of low κ and positive γ, respectively. The maximum and average relative errors between the numerical results and the correlations were: 17.5% and 2.8% and 9.6% and 1.7% for eqns (21) and (22), respectively. These correlations offer more accuracy than eqn (20) at the expense of a smaller range of applicability.

4. Conclusions

The average Nusselt number due to mixed convection from an isothermal cylinder at arbitrary angles of attack was solved for numerically. The study covered a wide

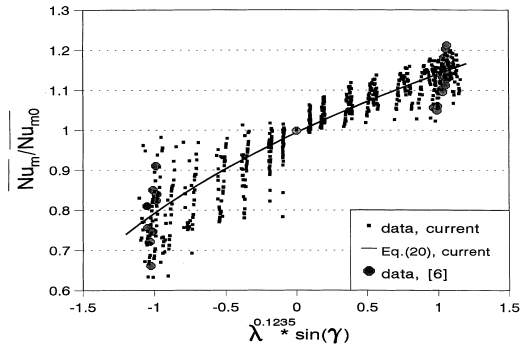

Fig. 6. Data points and correlation of normalized Nusselt number due to mixed convection at arbitrary angle of attack, full range of buoyancy parameter and angles of attack.

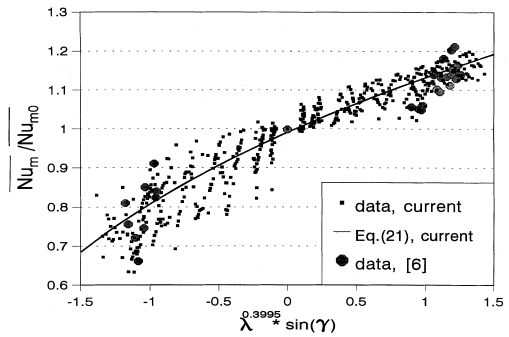

Fig. 7. Data points and correlation of normalized Nusselt number due to mixed convection at arbitrary angle of attack, $0 \leqslant \kappa \leqslant 10$.

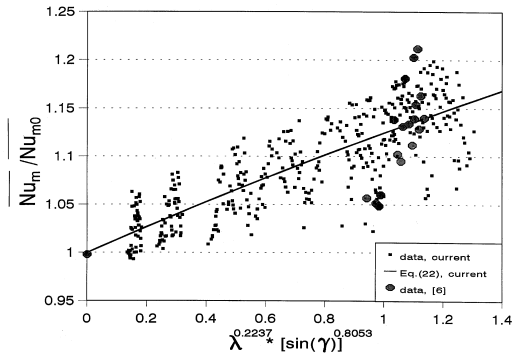

Fig. 8. Data points and correlation of normalized Nusselt number due to mixed convection at arbitrary positive angles of attack, $0 \leqslant \gamma \leqslant \pi/2$.

range of parameters: $1 \leqslant Re_D \leqslant 200$, $0 \leqslant \kappa \leqslant 35$, and $-\pi \leqslant \gamma \leqslant \pi$. Several correlations were proposed each with its own range of applicability. The error due to each correlation was also reported. These correlations enable engineers to predict the Nusselt number due to mixed convection from a cylinder subject to a wide range of conditions. The change in the average Nusselt number, relative to the case of cross flow, was up to (+20%) and (−30%) for aiding and opposing flows, respectively.

References

[1] B. Farouk, S.I. Guceri, Natural convection from a horizontal cylinder laminar regime, ASME Journal of Heat Transfer 103 (1981) 522–527.

[2] H.M. Badr, A theoretical study of laminar mixed convection from a horizontal cylinder in a cross stream, Int. J. Heat Mass Transfer 26 (1983) 639–653.

[3] M.W. Chang, B.A. Finlayson, Heat transfer in flow past cylinders at $Re < 150$—Part I. Calculations for constant fluid properties, Numerical Heat Transfer 12 (1987) 179–195.

[4] R.A. Ahmad, Z.H. Qureshi, Laminar mixed convection from a uniform heat flux horizontal cylinder in a crossflow, Journal of Thermophysics and Heat Transfer 6 (1992) 277–287.

[5] E.M. Sparrow, L. Lee, Analysis of mixed convection about a horizontal cylinder, Int. J. Heat Mass Transfer 19 (1976) 229–231.

[6] A.P. Hatton, D.D. James, H.W. Swire, Combined forced and natural convection with low-speed air flow over horizontal cylinders, J. Fluid Mech 42 (1970) 17–31.

[7] H.M. Bard, Laminar combined convection from a horizontal cylinder-parallel and contra flow regimes, Int. J. Heat Mass Transfer 27 (1984) 15–27.

[8] V.T. Morgan, The overall convection heat transfer from smooth circular cylinder, Adv. Heat Transfer 11 (1975) 199–264.

[9] J.D. Anderson, Computational Fluid Dynamics: The Basics with Applications, McGraw Hill, New York, 1994.

[10] S.V. Patankar, Numerical Heat Transfer of Fluid Flow, McGraw-Hill, New York, 1980.

[11] R.A. Ahmad, Steady-state numerical solution of the Navier–Stokes and energy equations around a horizontal cylinder at moderate Reynolds numbers from 100 to 500, Heat Transfer Engineering 17 (1996) 31–81.

[12] F.P. Incropera, D.P. DeWitt, Fundamentals of Heat and Mass Transfer, John Wiley & Sons, New York, 1996.

[13] A. Isaji, O. Tajima, Mass transfer from humid air to a circular cylinder in cross flow, Heat Transfer—Jap Res. 2 (1973) 12–24.